Ca^{2+} Concentration Dynamics in Spatially Extended Cells Physics 171/271

Flavio Fröhlich (flavio@salk.edu)

December 1, 2006

While previous lectures have been mostly concerned with neuronal dynamics derived by averaging over temporal and spatial scales to capture global behavior, we return to a biologically relevant subcellular spatial inhomogeneity, specifically to temporal and spatial dynamics of intracellular $[Ca^{2+}]$. Main interest in intracellular $[Ca^{2+}]$ derives from the fact that $[Ca^{2+}]$ acts as a second messenger and is crucially involved in a broad range of synaptic plasticity forms. Moreover, so-called calcium sensitive dyes, calcium buffers which change their fluorescent properties in response to calcium-binding, are widely used to optically probe neural acitivity. This class is separated intro three sections[1]. In the first section, we will look at the dynamics of buffer/calcium interaction neglecting the spatial scale (no diffusion). The second section contains the derivation of the so-called reaction-diffusion equation where we extend the findings from the first section by adding diffusion. The third and last section shows how a simple version of the previously described equations can be used to interprete important experimental results which indicate that synaptic spines represent diffusional compartments.

1 Calcium Buffering

Since $[Ca^{2+}]$ plays such a vital role in intacellular signaling, calcium buffers in neurons tightly regulate the calcium concentration. So we start with reviewing a basic first order chemical reaction which describes the interaction of calcium $[C]$ with a buffer $[B]$

$$[C] + [B] \rightleftharpoons [CB] \tag{1}$$

Note that buffer bound to calcium is denoted by $[CB]$ and that the reaction is defined by the on and off rate constants k_1 (binding) and k_2 (unbinding), respectively. The total amount of buffer denoted by $[B_T]$. The reaction is then described by

$$\frac{d[C]}{dt} = k_2[CB] - k_1[C][B] \tag{2}$$

[1]Main soruces are (Yasuda et al. 2004),(Zador and Koch 1994), and the previous year's handouts.

where the total amount of buffer is the sum of the unbound and bound buffer:

$$[B_T] = [B] + [CB] \tag{3}$$

We can now determine the steady-state solution of this differential equation. We eliminate [B] by setting the derivative to zero and solving for [CB].

$$[CB] \quad = \frac{[C][B_T]}{[C]+k_d} \tag{4}$$

We have introduced the dissociation constant $k_d = k_2/k_1$ which is called the dissociation constant:

$$k_d = \frac{[B][C]}{[BC]} \tag{5}$$

Thus, high values of k_d describe buffers with limited ability to bind to its ligand.

After having worked out the basics, we turn our attention to a simple model of intracellular calcium [Ca^{2+}] in presence of an endogenous ("natural") calcium buffer and an exogenous calcium buffer (e.g. calcium dye). In this model, we sum the calcium entering and leaving the compartment/cell to keep track of the changes in total calcium concentration $[Ca^{2+}]_T$:

$$\frac{d[Ca^{2+}]_T}{dt} = \frac{i(t) - e(t)}{V} \tag{6}$$

Since we are specifically interested in the free calcium concentration, we assume a sufficient separability of time-scales, meaning that the interaction of the calcium with buffers is much faster than the in- and outflux of calcium.

$$\frac{d[Ca^{2+}]_T}{dt} = \frac{d[Ca^{2+}]}{dt} + \frac{d[BC]}{dt} + \frac{d[DC]}{dt} = (1 + \kappa_B + \kappa_d)\frac{d[Ca^{2+}]}{dt} \tag{7}$$

Where we have used the chain rule of differention (details of this elimination of the fastest time-scale are given in the next section):

$$\kappa_X = \frac{K_d X_T}{(K_d + [Ca^{2+}])^2} \tag{8}$$

Remember that this is the steady state condition for the buffering, thus we find:

$$\frac{d[Ca^{2+}]}{dt} \quad = \quad \frac{1}{\beta V}\left(i(t) - e(t)\right) \tag{9}$$

$$\beta \quad = \quad 1 + \kappa_B + \kappa_D \tag{10}$$

Let us now assume that the extrusion $e(t)$ is proportional with constant Γ to the elevation of calcium above baseline $[Ca^{2+}]_o$:

$$e(t) = \Gamma([Ca^{2+}] - [Ca^{2+}]_o) \tag{11}$$

As a result, we get a first order differential equation with an inhomogenous current $i(t)$ with solution

$$[Ca^{2+}](t) = \int_0^t d\tau \frac{i(\tau)}{\beta V} \exp\left(-\frac{\Gamma}{\beta}(t-\tau)\right) + [Ca^{2+}]_o \tag{12}$$

If we model the calcium influx elicited by an action potential as a delta function with total amount of charge Q, the solution is then given by

$$[Ca^{2+}] = \frac{Q}{\beta V} \exp\left(\frac{-\Gamma}{\beta}t\right) + [Ca^{2+}]_o \tag{13}$$

2 Calcium Buffering with Diffusion

We now include difussion of both calcium and buffer in the above derivation. We will find the so-called reaction-diffusion equation. We start with the diffusion equation

$$\frac{\partial C(x,t)}{\partial t} = D\frac{\partial^2 C(x,t)}{\partial x^2} + \frac{2}{a} \tag{14}$$

We now include a simple first order calcium buffer rate equation. We will then make use of the different time-scales, namely that calcium buffering works on a much faster time scale than changes in calcium concentration mediated by diffusion, influx, and extrusion by pump. The singularly perturbed system is:

$$\begin{aligned} \frac{\partial C(x,t)}{\partial t} &= D\frac{\partial^2 C(x,t)}{\partial x^2} - P(C) - fCB - bM + \frac{2}{a} && (15)\\ \frac{\partial M}{\partial t} &= D_b\frac{\partial M}{\partial x^2} + fCB - bM && (16)\\ B_T &= M(x,t) + B(x,t) && (17) \end{aligned}$$

Note that we assume the same diffusion constant D_b for both the bound and unbound buffer. The pumps is activity dependent, follows a sigmoidal nonlinearity, and saturates at P_m:

$$P(C) = \frac{2P_m}{a}\frac{C}{1 + C/K_p} \tag{18}$$

Since we will later linarize this equation, let us consider the low concentration ($C << K_p$) and high concentration ($C >> K_p$) limits. In the previous, we find $P(C) = (2P_m C)/(a)$, whereas in the later $P(C) = (2P_m K_p)/a$.

We now turn our attention to the equation governing the dynamics of the bound buffer M since we want to eliminate its fastest time-scale. For that, we drop the diffusion term (we will reintroduce it later), by setting: $D_b = 0$:

$$\frac{\partial M}{\partial t} = fCB - bM \tag{19}$$

Note that we here hold calcium concentration C constant. Using $B_T = M + B$, we find a first order differential equation with usual exponential relaxation solution:

$$M(t) = M_\infty + (M_0 - M_\infty)e^{-\frac{t}{\tau_b}} \tag{20}$$

where the steady state solution is:

$$M_\infty = \frac{B_T C}{K_d + C} \tag{21}$$

We can now separate out the change in bound buffer concentration mediated by change in calcium concentration and the change in buffer concentration due to the binding dynamics for a given fixed calcium concentration. Remember that have assumed the latter to be instantaneous (elimination of fastest time scale):

$$\frac{\partial M}{\partial t} = \frac{\partial M}{\partial C}\frac{\partial C}{\partial t} = \frac{B_T K_d}{(K_d + C)^2} = -fCB + bM \tag{22}$$

This can now be plugged into the partial differential equation for $C(x,t)$:

$$\left(1 + \frac{B_T K_d}{(K_D + C)^2}\frac{\partial C}{\partial t}\right) = D\frac{\partial^2 C}{\partial x^2} - P(C) \tag{23}$$

Note that this equation has some ugly non-linearity in state variable C. We first introduce the following abbreviation

$$\beta = \frac{B_T K_d}{(K_D + C)^2}, \tag{24}$$

for which we now determine the low concentration limit where $C << K_d$.

$$\beta = \frac{B_T}{K_d} \tag{25}$$

Using the previously determined linarization fo the calcium pump $P(C)$, we find after some final polishing:

$$\frac{a}{2}(1+\beta)\frac{\partial C(x,t)}{\partial t} = \frac{a(D + \beta D_b)}{2}\frac{\partial^2 C}{\partial x^2} - P_m C + i(x,t) \tag{26}$$

Note that we have hereby derived the reaction-diffusion equation. A comparison reveals strong similarity with the linear cable equation:

$$c_m \frac{\partial V(x,t)}{\partial t} = \frac{a}{2r_i} \frac{\partial^2 V(x,t)}{\partial x^2} - \frac{1}{R_m} V(x,t) + i_2 \tag{27}$$

We can therefore make use of our prior analysis of the linear cable equation and determine in complete analogy the chemical time and space constants τ_c and λ_C:

$$\tau_c = \frac{a(1+\beta)}{2P_m} \tag{28}$$

$$\lambda_c = \sqrt{\frac{a(D+\beta D_b)}{2P_m}} \tag{29}$$

3 Spines form Diffusional Compartments

This section is concerned with the Ca^{2+} dynamics in *spines*, which are protrusions of the neural cell membrane. A typical spine consists of a head (volume 0.001-1 μm^3) and a (in most cases) thin neck (diameter < 0.1 μm). More than 90% of all excitatory synapses terminate on spines, making spines a vastly abundant structure in the central nervous system. The spatial scale requires serial electron miscroscopy to recover the ultrastructure. Recent developments in two photon laser microscopy in combination with calcium-sensitive dyes allow for Ca^{2+} measurements in spines with high temporal and spatial resolution. While this lecture is not further concerned with the phenomenology, it should be mentioned that there are a series of highly interesting findings concerning plasticity via structural changes of spines and concerning the implication of altered spine distribution and morphology in a series of both congenital and infectuous neurological disorders.
Intuitively it is clear, that such subcellular structure can potentially mediate spatial specificity of dendritic information processing. In the following, we will discuss a simple model which was used to interprete experimental data answering the question whether spines represent diffusional compartments.

Figure 1: Mushrooms in physics (left) and biology (right)

Two main methods have been used to determine the diffusional coupling between the spine head and the dendrite from which the spine neck originates. Here, we first discuss diffusion measurements by *fluorescence recovery after photbleaching (FRAP)*. Basic idea is that a cell (including its spines) is loaded with a freely diffusable fluophore such that at baseline the fluophore concentration as measured by its fluoresence is equal in the spine and in the dendritic shaft. In mathematical notation, we describe the baseline state as follows:

$$C_h(t=0) = C_s(t=0) \tag{30}$$

Laser pulses are used to alter C_h by photobleaching. Then, the time-course of $C_h(t)$ converging back to baseline fluorescence is measured. The estimation which we develop here is based on the following two insights/assumptions:

1. The spinehead is sufficiently small in volume that we can assume intraspinehead diffusion to be instantaneous.

2. The dendritic shaft concentration $C_s(t)$ is assumed to be constant, implying that any changes related to the recovery of baseline $C_h(t)$ are minute in comparison to $C_s(t=0)$.

Measurements were found to show first-order recovery dynamics, which can be explained by the following simple model. Let's assume that there is constant flux in the spine neck of geometry with cross-section A and length l. The flux $J(t)$ is then proportional to the concentration gradient:

$$J(t) = D\frac{C_h(t) - C_s}{L}. \tag{31}$$

Remember that flux $J(t)$ is proportional to the change rate of concentration, giving:

$$J(t)A = -V_h\frac{C_h(t)}{dt}, \tag{32}$$

where V_h denotes the volume of the spine head and A the cross-section of the neck. We can now combine these equations to find:

$$\frac{C_h(t)}{dt} + \left(\frac{AD}{LV_h}\right) C_h(t) = \left(\frac{AD}{LV_h}\right) C_s \tag{33}$$

Note that this a simple first order differential equation for which we can immediately write down the solution:

$$C_h(t) = C_s + \Delta C_h(0) e^{-\frac{LV_h}{AD}t}. \tag{34}$$

In the experiment, time constant $\tau = \frac{LV_h}{AD}$ was measured. Since we can termine the volume by optical sectioning, we can compute the ratio of length to area of the spine head:

$$\frac{A}{L} = \frac{V_h}{\tau D} \tag{35}$$

Importantly, the experimentally determined time constant τ is in the range of 20-200 msec, thus indicating that indeed diffusional exchange between spine head and dendritic shaft is slow in comparison to time constants of intracellular biochemical signalling. Since we specifically consider Ca^{2+} ins this lecture, it is important to note that free Ca^{2+} has a similar difussion coefficient to the used fluophore.

The concern that photobleaching could introduce artefacts in the above described experiments, an alternative approach based on *optical fluctuation analysis* has also been used, leading to similar results. These experiments are based on the fact that a postsynaptic action potential leads to stochastic opening of voltage-gated calcium channels located on the spine surface resulting in trial-by-trial calcium concentration variability. This variance is dissipated by diffusion of Ca^{2+} across the spine neck. We can thus measure the decay time constant of the trial-by-trial variability in of $C_h(t)$ to determine the diffusion time constant. Specifically, we make use of the linearity of the averaging operation and find:

$$\frac{d\langle C_h(t)\rangle}{dt} = \frac{1}{\tau}(\langle C_d(t)\rangle - \langle C_h(t)\rangle), \tag{36}$$

noting that the average is an average over a set of trials (and not time). Experimentally determined low trial-to-trial varaibility in the dendrite permits:

$$\langle C_d\rangle \approx C_d. \tag{37}$$

We can now subtract to find the following differential equation:

$$\frac{d(C_h - \langle C_h\rangle)}{dt} = -\frac{1}{\tau}(C_h - \langle C_h\rangle). \tag{38}$$

The solution is again a simple first order exponential time-course. We can then determine thereof the time-course of the variance:

$$\sigma_h^2 = \sigma^2(0) e^{-\frac{2t}{\tau}}. \tag{39}$$

Note the factor of two in this result.

We thus answer the question whether spines form diffusional compartments with *yes*.

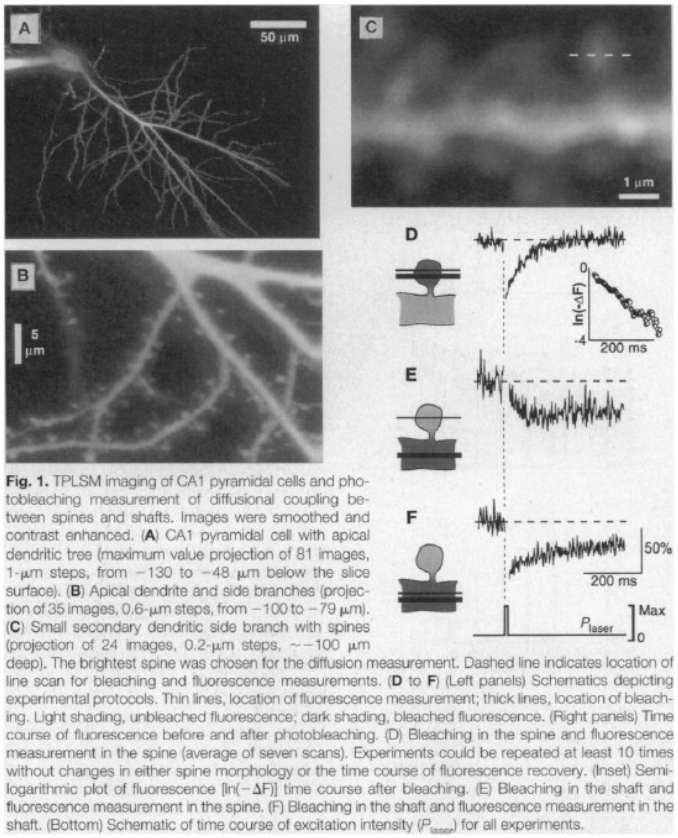

Fig. 1. TPLSM imaging of CA1 pyramidal cells and photobleaching measurement of diffusional coupling between spines and shafts. Images were smoothed and contrast enhanced. (**A**) CA1 pyramidal cell with apical dendritic tree (maximum value projection of 81 images, 1-μm steps, from −130 to −48 μm below the slice surface). (**B**) Apical dendrite and side branches (projection of 35 images, 0.6-μm steps, from −100 to −79 μm). (**C**) Small secondary dendritic side branch with spines (projection of 24 images, 0.2-μm steps, ~−100 μm deep). The brightest spine was chosen for the diffusion measurement. Dashed line indicates location of line scan for bleaching and fluorescence measurements. (**D** to **F**) (Left panels) Schematics depicting experimental protocols. Thin lines, location of fluorescence measurement; thick lines, location of bleaching. Light shading, unbleached fluorescence; dark shading, bleached fluorescence. (Right panels) Time course of fluorescence before and after photobleaching. (D) Bleaching in the spine and fluorescence measurement in the spine (average of seven scans). Experiments could be repeated at least 10 times without changes in either spine morphology or the time course of fluorescence recovery. (Inset) Semilogarithmic plot of fluorescence [ln(−ΔF)] time course after bleaching. (E) Bleaching in the shaft and fluorescence measurement in the spine. (F) Bleaching in the shaft and fluorescence measurement in the shaft. (Bottom) Schematic of time course of excitation intensity (P_{laser}) for all experiments.

Figure 2: FRAP experiment (Svoboda at al. 1996).

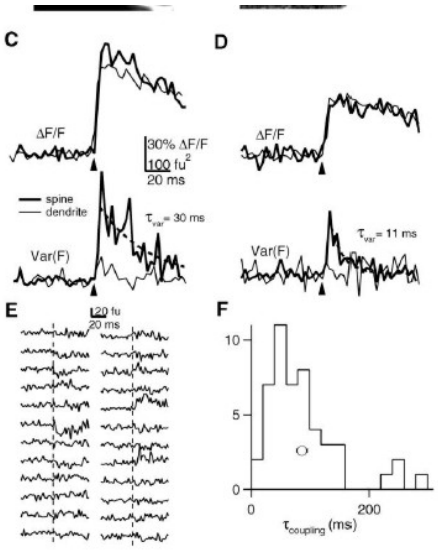

Figure 4. Diffusional Equilibration of Ca^{2+} across the Spine Neck Measured with Optical Fluctuation Analysis

(A and B) Examples of dendritic spines.

(C) Average $(\Delta F/F)_{AP}$ (top, 66 trials) in the spine (thick) and parent dendrite (thin) for spine shown in (A). The variance of the fluorescence transients due to fluctuations in $[Ca^{2+}]$ in the spine and dendrite are shown below. Superimposed is an exponential fit to the decay of the variance in the spine (dashed line).

(D) Average $(\Delta F/F)_{AP}$ (top, n = 50) and variance of the fluorescence transient due to fluctuations in $[Ca^{2+}]$ (bottom) for the spine and parent dendrite shown in (B).

(E) Deviations from the mean for 24 sequential trials of $(\Delta F/F)_{AP}$. Dashed lines indicate the time of somatic current injection.

(F) Histogram of τ_{equi} measured from 49 spine/dendrite pairs. The mean τ_{equi} ± SEM is also indicated.

Figure 3: Optical fluctuation analysis (Sabatini et al. 2002).